Ion-implantation of erbium into the nanocrystalline diamond thin films

P. NEKVINDOVÁ[a], O. BABCHENKO[d], J. CAJZL[a], A. KROMKA[d], A. MACKOVÁ[b,c], P. MALINSKÝ[b,c], J. OSWALD[d], V. PRAJZLER[d,e], Z. REMEŠ[d], M. VARGA[d]

[a]*Department of Inorganic Chemistry, University of Chemistry and Technology, Prague 166 28, Czech Republic*
[b]*Nuclear Physics Institute, Academy of Sciences of the Czech Republic, v.v.i., 250 68 Řež, Czech Republic*
[c] *Department of Physics, Faculty of Science, J. E. Purkinje University, České mládeže 8, 400 96 Ústí nad Labem, Czech Republic*
[d] *Institute of Physics, Academy of Sciences of the Czech Republic, v.v.i., Cukrovarnická 10, 162 00 Prague, Czech Republic*
[e] *Department of Microelectronics, Faculty of Electrical Engineering, Czech Technical University in Prague, Technická 2, 166 27 Prague 6, Czech Republic*

High-refractive-index nanocrystalline diamond films deposited on borosilicate glass from a $CH_4/CO_2/H_2$ gas mixture by a linear-antenna microwave plasma-enhanced chemical vapour deposition (MW PECVD) were doped by erbium using ion-implantation technique. The prepared thin films guided an optical signal in the range of 632–1552 nm and revealed measurable luminescence around 1530 nm. The changes of optical properties and surface morphology were studied more in detail.

(Received April 4, 2016; accepted August 3, 2016)

Keywords: Nanocrystalline diamond, Optical waveguides, Erbium, Luminescence, Ion implantation, CVD

1. Introduction

Nanocrystalline diamond (NCD) represents a new material that retains the outstanding material properties of single-crystalline diamond. Moreover, thin NCD films can be used for photonic applications due to unique optical properties [1,2]. Besides the low absorption scattering over a broad spectrum, these properties include a very high refractive index (approximately 2.39 for a wavelength of 1310 nm), which means that this material deposited on silica glass or a silica-on-silicon substrate can be used for high-index-contrast (HIC) waveguides [3,4]. Intentional doping of diamond with impurity atoms (e.g., silicon, nitrogen or chromium) can produce a range of colour-defect centres with strong and stable luminescence, no photobleaching and long quantum coherence times [5]. These centres can be artificially engineered in the diamond lattice during the growth process or post-processing by ion implantation [6-8]. Nowadays, the increase/decrease in the number of the nitrogen- and silicon-vacancy (N-V and Si-V, respectively) centres in mono- and polycrystalline diamond as a function of process parameters and/or implantation is being studied in detail [9,10].

This paper presents the study on doping of thin NCD films with erbium ions to create erbium (Er) luminescence centres in diamond waveguides in order to fabricate new material for active photonic structures. The relations between the virgin and as-implanted film morphologies, waveguiding and luminescence properties are also discussed.

2. Experiments

Prior to the diamond growth, Corning Eagle2000 borosilicate glass (10×10 mm^2) was seeded by applying an ultrasonic agitation in water-based diamond-powder (NanoAmando, New Metals and Chemicals Corp. Ltd., Kyobashi) suspension. Diamond films were grown by a pulsed linear-antenna microwave plasma CVD process (modified system AK 400, Roth and Rau, AG) from the $CH_4/CO_2/H_2$ gas mixture. The diamond-growth conditions were: 2.5 % of CH_4 and 10 % of CO_2 compared with hydrogen, 2x pulsed microwave power of 2 kW, the deposition time of 18 hours and the substrate temperature of 650 °C. Two different sets of diamond films were grown by controlling the total gas pressure alone during the diamond growth. The smaller-grain sized diamond film was deposited at a gas pressure of 100 Pa and the larger-grain sized diamond film at a pressure of 8 Pa. The decrease in the gas pressure resulted in a more effective plasma spreading in the vacuum chamber, which further led to the growth of the diamond film with higher optical quality (fewer sp^2 phases) [11].

For the ion implantation, the NCD films mentioned above as well as single-crystalline diamond substrates

(3×3×0.1 mm) with ⟨001⟩ crystallographic orientation were used. Thoroughly pre-cleaned samples were implanted by 190 keV Er^+ ions. The ion implantation fluence of 1.0×10^{14} cm^{-2} was used.

The surface morphology and grain size of the deposited diamond films were studied by scanning electron microscopy (SEM). The diamond phase distribution was studied by a Renishaw InVia Reflex Raman spectrometer with the excitation wavelength of 442 nm. The topography of the NCD films was investigated by atomic force microscopy (AFM) in the PeakForce QNM mode by using CF_4 plasma treated Multi75Al cantilever. The diamond-film thickness was evaluated from the interference fringes in the reflectance spectra measured in the UV-VIS-NIR region using commercial software for the modelling of the optical properties of thin films (Film Wizard™).

The Er concentration depth profiles of the incorporated erbium were measured by Rutherford Backscattering Spectroscopy (RBS). The analysis was performed at Tandetron 4130 MC accelerator using a 2.0 MeV He^+ ion beam. The data collected were evaluated and transformed into Er concentration depth profiles using the GISA 3.99 [12] and SIMNRA 6.06 [13] codes, utilizing cross-section data from IBANDL [14]. The degree of damage introduced by the ion implantation process on the host lattice was examined by RBS/channelling measurements using a 1.7 MeV He^+ beam at Van de Graaff accelerator.

The waveguiding properties of NCD planar waveguides were characterized by the Metricon 2010 prism-coupler system. The apparatus works on the principle of the dark-mode spectroscopy [15] (see [16] for a detailed description). The measured wavelengths were in the range from 473 to 1552 nm.

The photoluminescence spectra of the prepared samples were collected within the range of 1440–1600 nm at room temperature. A pulse semiconductor laser POL 4300 emitting at 980 nm was used for the excitation.

3. Results

The diamond films were characterized in terms of their morphology as well as their phase distribution. Moreover, the root-mean-square (RMS) roughness, absorbance, waveguiding and luminescence properties of the films were determined. Results from all the measurements are summarized in Table 1. The SEM images, the Raman spectra and the AFM images of the as-grown diamond films are shown in Fig. 1. The Raman spectrum consists of three main peaks. The peak at 1150 cm^{-1} as well as shoulder at 1480 cm^{-1} are assigned to trans-polyacetylene which is characteristic for NCD and UNCD (Ultra-nanocrystalline diamond) films. Single-crystal diamond has characteristic peak at 1332 cm^{-1} (sp^3 carbon coordination), while single–crystal graphite has a peak at 1580 cm^{-1} (sp^2 carbon coordination). The shoulder at 1350 cm^{-1} (D-band) corresponds to the "disordered" or glassy carbon structure (sp^2 carbon coordination) [17-19].

The lower deposition pressure (8 Pa) resulted in plasma spreading in the vacuum chamber closer to the substrate and consequently enhanced the reactions at the substrate surface. Moreover, it caused an increase in the diamond growth rate and also more effective etching of the sp^2 phases. Such a diamond film has larger grains, i.e. fewer grain boundaries, in comparison with the diamond film deposited at the total gas pressure of 100 Pa. On the other hand, the surface roughness increased four times. In the case of the smaller grains and thus higher number of grain boundaries with sp^2 phases, the absorbance at the wavelength of 1240 nm increased almost seven times [20]. The Raman spectra, as well as AFM analysis, did not show any changes between Er implanted and non-implanted samples. Since the depth of Raman spectra measurement was of about 1 μm, the assumed graphitization of the thin surface layer (approx. 100 nm) of the implanted samples was not apparent in the spectra.

Table 1. A comparison of the selected properties of thin NCD films deposited on a glass substrate using various deposition pressures (8 and 100 Pa) for as grown (A, B) and Er-implanted (Ai, Bi) samples.

Sample	Grain size [nm]	RMS roughness [nm]	Absorbance (at 1240 nm) [rel. %]	Waveguiding at 633 nm
A – 8 Pa	>100 nm	~20	0.3	Yes
B –100 Pa	<25 nm	~5	2	No
Ai – 8 Pa	>100 nm	~20	-	Yes
Bi – 100 Pa	<25 nm	~5	-	No

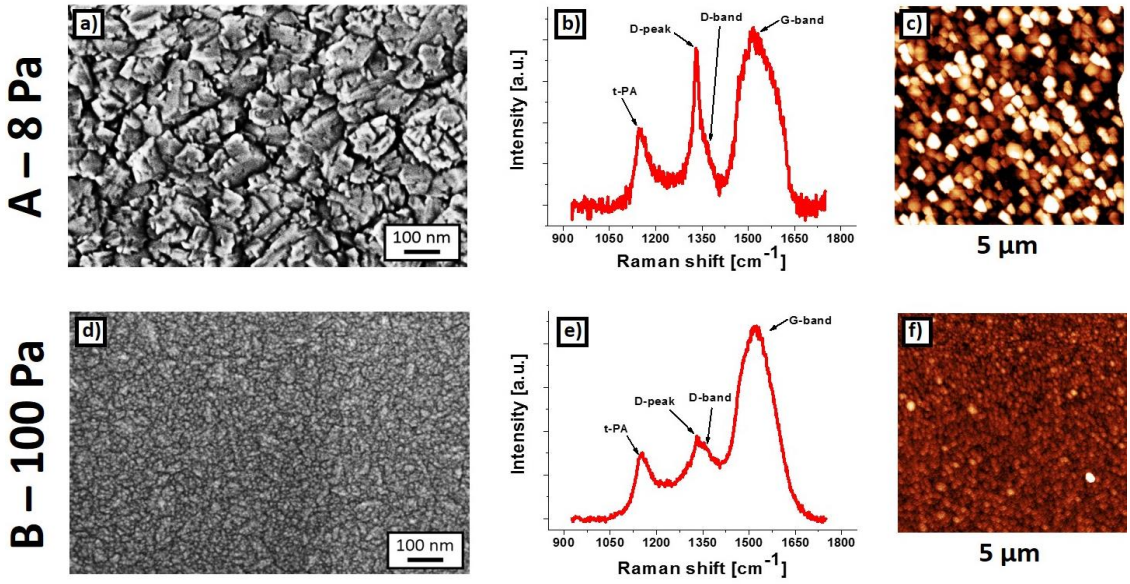

Fig. 1. The SEM images, the Raman spectra and the AFM images (5×5 µm^2, Z-scale ~50 nm) of the as-grown diamond films deposited using the total gas pressure of 8 Pa (a, b and c) and 100 Pa (d, e and f).

The thicknesses of the prepared films were determined by evaluation of interference fringes in the reflectance spectra and by mode spectroscopy of the waveguiding films. Using the reflectance spectra, the film thicknesses of the larger-grain (A – 8 Pa) and smaller-grain (B – 100 Pa) sized diamond films were estimated to be 400 nm and 250 nm, respectively. Using the mode spectroscopy, the thickness of 401 nm was determined for the sample A – 8 Pa; the sample B – 100 Pa could not be measured, most probably due to the strong absorption. Comparing the thickness measurement results of both methods for the sample A – 8 Pa it is evident that both methods are in good agreement.

Using dispersion equation [21], it is possible to calculate the waveguiding properties of the prepared films, i.e. the number of guided modes and the pertinent refractive index value. It means that using data for the wavelength of 633 nm (i.e. the refractive index of the prepared diamond film of 2.36, the film thickness of 400 nm, and the refractive index of the glass substrate of 1.46), it was calculated that the fabricated planar waveguide will guide three optical modes. The first one would correspond to the refractive index of 2.265, the second one to 2.016 and the third one to the value of 1.573 for the TE (transverse-electric) light polarisation. Although the step-index like profile was expected, the last mode has the refractive index similar to the glass substrate value. Fig. 2 shows calculated modes (2a) as well as the measured data (2b). The measured values of the refractive indices for the wavelengths of 473 – 1552 nm are summarized in Table 2. The measured refractive indices associated with the particular modes are in a very good agreement with the first two values calculated by the dispersion equation. The third mode was not present in the measured mode spectrum, because it would occur at the refractive index of about 1.57 which is outside of the measuring prism range.

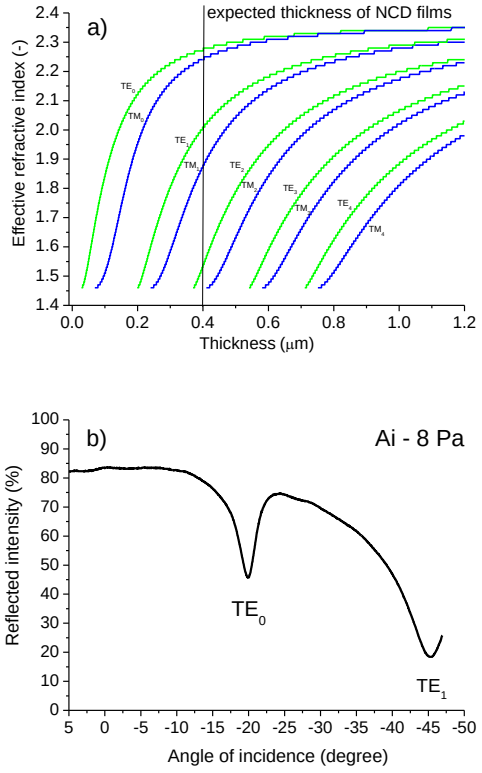

Fig. 2. The calculated (a) as well as measured data (b) of the optical modes. The calculation was done at a wavelength of 633 nm. The spectrum, where the position of particular modes is evident, was measured on the Er-implanted diamond film Ai – 8 Pa.

From the comparison of the waveguiding properties of the larger-grain (A – 8 Pa) and smaller-grain (B – 100 Pa) sized diamond films (see Table 1) it is clear that the strong absorption in the grain boundaries of smaller-grain sized film (B – 100 Pa) could be attributed to the higher amount

of grain boundaries when compared to the large-grained sample. The waveguiding properties of the large-grain sized as-grown film (A – 8 Pa) and as-implanted film (Ai – 8 Pa) are summarized in Table 2. These results clearly show that the optical signal has been guided for wavelengths longer than 633 nm. The two measured optical modes at a wavelength of 633 nm allowed calculating the deposited film thickness. Consequently, the thickness value of 400 nm was further used for the calculation of the refractive index value for larger wavelengths where only one optical mode was found. As expected, the refractive index values decreased with the longer wavelengths and were in the range of 2.362–2.339 for the as-grown NCD. The number of guided modes as well as the refractive index values were in very good agreement with the theoretical calculations.

Table 2. The waveguiding properties of as-grown and as-implanted larger-grain sized thin NCD films

Sample	**A – 8 Pa** as-grown		**Ai – 8 Pa** as-implanted	
Wavelength [nm]	Number of modes	Refr. index [-]	Number of modes	Refr. index [-]
473	0	-	0	-
633	2	2.3617	2	2.3446
964	1	2.3442*	1	2.3185*
1311	1	2.3398*	1	2.3094*
1552	1	2.3394*	1	2.3036*

*The assumed values based on the calculation of thickness at the 633 nm wavelength; the values of the determined thicknesses were 401 nm and 418 nm for the A – 8 Pa and Ai – 8 Pa samples, respectively.

Moreover, the results summarized in Table 2 clearly confirm that both as-grown and Er-implanted larger-grain sized films (Ai – 8 Pa) have similar waveguiding properties – the as-implanted waveguide has the same number of modes in contrast with the refractive index decrease of approximately 1.3%.

The two fabricated NCD samples along with monocrystalline diamond were implanted with erbium ions using the same experimental conditions. Subsequently, the concentration depth profiles of implanted Er were measured by RBS. The positions of incorporated erbium ions in the single-crystal diamond were measured by RBS/channelling. Moreover, the Er-concentration depth profiles were compared to the SRIM 2012 simulations, which predicted Er-ion ranges and stragglings using MC simulations [22]. The results are presented in Fig. 3a with the given erbium concentration depth profiles in the single-crystalline diamond as well as the profile of the NCD film with larger grains (sample Ai – 8 Pa).

The simulated projected ranges (R_p) and range stragglings (ΔR_p – the standard deviation of the projected range of ions) of Er were similar in the NCD film and single-crystal diamond (the R_p is 40 nm and the ΔR_p is 7 nm), as we supposed from the same compositions and densities of the materials. However, experimentally measured Er concentration depth profiles showed in the single-crystalline diamond the maximum concentration depth R_p *(diamond)* of 42 nm and the standard deviation of the Er concentration depth profile ΔR_p *(diamond)* of 12 nm, while in the as-implanted NDC film, we observed the R_p *(NCD)* of 36 nm and the ΔR_p *(NCD)* of 13 nm. The Er concentration depth profile of the NCD film had a higher maximum Er concentration in the projected range depth and the narrower depth profiles as compared to the single-crystalline diamond.

Regarding the relatively low ion fluence used, RBS measurements confirmed a low erbium concentration – the max. of 0.04 at. %. Erbium concentration depth profiles were similar for both types of the samples. The maximum erbium concentration depths were very close to the projected range value predicted by SRIM [22]. The values of erbium concentration determined by RBS differed for the samples of single crystal diamond and NCD. The reason for this could be the extremely low erbium concentration near the detection limit of RBS (approx. 0.005 at. %), which can cause a higher inaccuracy of the evaluated results.

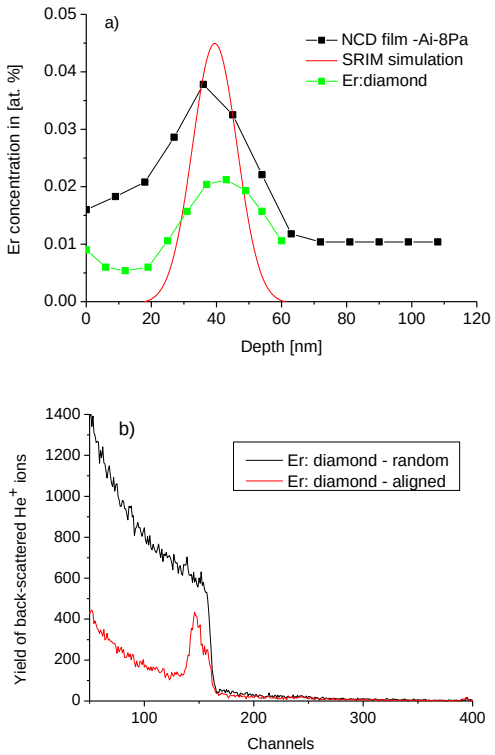

Fig. 3. The concentration depth profiles of the erbium-doped NCD films and diamond single-crystal with the SRIM simulation (a) and the RBS channelling spectra of erbium-doped diamond single-crystal (b).(Experimental conditions: 190 keV Er^+ ions, fluence of 1.0×10^{14} cm^{-2}).

From a comparison of random and aligned RBS/channelling spectra of diamond single crystal, measured along the same crystal axes, it can be deduced that approx. 30 % of the carbon atoms are displaced from their original positions. In NCD films, the disordered atom density cannot be determined by RBS/channelling since the main principle of ion channelling (focused ion beam aligned in the string potential of the ordered nuclei in the single-crystal material) applies only in strongly long-range-ordered structures such as single crystals.

A comparison of the baseline-corrected photoluminescence spectra of the erbium-implanted NCD films and the single-crystalline diamond is provided in Fig. 4. Although we did not expect high luminescence intensity due to the small erbium implantation dose (and also due to the atomic vibration noise caused by the measurement done at room temperature), we surprisingly found two broad luminescence bands with the maxima at 1481 and 1530 nm. The luminescence was detected in the NCD sample (Ai – 8 Pa), which had a lower number of grain boundaries. For the single-crystal structure as well as for samples with smaller grains (Bi – 100 Pa) no luminescence was observed. According to these results, we think that certain density of grain boundaries is not suitable to achieve luminescence emission around 1.5 μm (emission transitions between $I_{13/2}$ and $I_{15/2}$ energy sublevels of erbium ions).

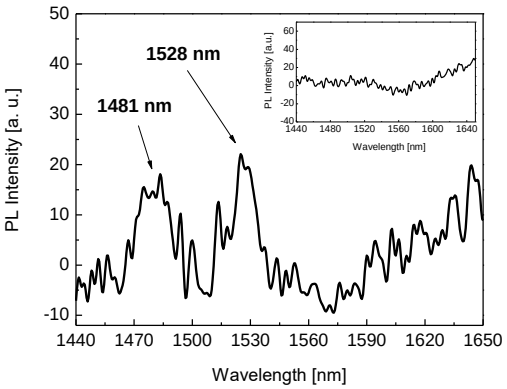

Fig. 4. The luminescence spectra of the erbium-doped NCD film (Ai – 8 Pa) and of the the erbium-doped diamond single-crystal (100) sample (inset graph). (Experimental conditions: 190 keV Er^+ ions, a fluence of 1.0×10^{14} cm^{-2}.

4. Discussion

The Raman spectra clearly show that when the lower pressure is applied during the thin film growth process the amount of sp^3 phase rise (obviously some peaks are broadened due to the various crystallite sizes and thicknesses). The similar trends were observed for example in [18,19].

Moreover, the NCD films prepared with lower pressure exhibited guiding of the optical signal for wavelengths ranging from 633 to 1550 nm. The ion implantation process affected the waveguiding properties negligibly. Since the NCD films exhibited high optical absorption (most probably due to the optical dispersion on grain boundaries) it has been found that for the sufficient optical waveguiding (regarding the mentioned wavelengths) the grain sizes should be larger than 100 nm. Samples with smaller grains significantly increased the optical absorption; therefore such films cannot sufficiently transmit the optical signal.

From the literature the similar diamond waveguide structures have been rarely prepared by different methods on various substrates [23,24,25]. We found only two groups where the waveguiding properties of NCD films were described. If we compare the results with the published ones [23,24] it is evident that the films prepared by our group are thinner but the refractive index value is for the same wavelengths practically the same (the difference is about 0.02 for the wavelength of 633 nm). The advantage of thin NCD films prepared by our group is the high contrast of refractive index values which is allowing for the thinner NCD films that can be used as HIC optical waveguides in photonics.

The erbium luminescence at around 1530 nm was observed in the samples with larger grains (and thus lower amount of grain boundaries). For a good luminescence properties (i.e. mainly narrow peaks with high intensities) it is important that the incident erbium ions transform into Er^{3+} ions because erbium in the form of Er^{3+} in the structure implies favourable distribution of erbium ions and low tendency to form erbium clusters (erbium in oxidation state zero) that cause luminescence quenching. Also the coordination of erbium in the crystal structure is very important. Therefore, the reason for the higher measured luminescence emission intensity of the larger-grain sized sample is probably the better distribution of erbium in the form of Er^{3+} in the large diamond grains, since the higher number of grain boundaries means higher degree of disorder in erbium surrounding.

To our knowledge this is the first time when the luminescence of erbium in the NCD diamond was registered and analysed. From the literature the only similar study of doping of RE ions into the diamond thin films was done by group of A. Magyar, *et al.* [26]. They did the theoretical as well as experimental study of Eu ions doping into diamond thin films using electrostatically assembled europium (III) chelate molecules combined with CVD technique. The luminescence of Eu was however at around 620 nm which belongs to the VIS or very near IR region. The region of luminescence was therefore similar to the other known color centres in diamond that have been observed [27,28]. In contrast, our Er-doped NCD samples with the emission in NIR region at around 1.5 μm (i.e. the 3rd telecom window, the region used for optical digital information transmission).

In the future, it would be beneficial to focus the research on using higher fluences of implanted erbium as well as on the structure modification of the diamond substrate. This would allow for the preparation of the suitable micro-structural form of NCD that would guide optical signal and have well distributed erbium ions. Another task would be to test if the post-implantation

annealing may have beneficial effect on the distribution of erbium ions in the structure.

5. Conclusion

The prepared NCD thin films guided up to two optical modes in the range of 633–1552 nm. It was found out that for the waveguiding to occur the size of NCD grains of more than 100 nm should be used (according to experimental conditions used). The erbium ion implantation process affected the optical waveguiding properties negligibly – the value of refractive index of 2.3394 for 1552 nm decreased by approximately 1.3 % after the ion implantation process. The erbium implanted NCD samples with smaller concentration of grain boundaries (which correspond to the large grain sizes of < 100 nm) revealed measurable luminescence at around 1530 nm.

Acknowledgement

We acknowledge the Czech Science Foundation project GA 14-05053S. Some parts of this research were realised at the CANAM (Center of Accelerators and Nuclear Analytical Methods LM 2011019) infrastructure and has been supported by the projects SGS UJEP 15 0012 01. The ion implantation experiments were realized at Ion Beam Center of Helmholtz Zentrum, Dresden – Rossendorf, Germany under the proposal 15100225-ST.

References

[1] W. Yang, Nature Materials **1**, 253 (2002).
[2] L. Ondic, O. Babchenko, M. Varga, A. Kromka, J. Ctyroky, I. Pelant, Scientific Reports **2**(914), 1 (2012),
[3] C. Manolatou, S. G. Johnson, S. Fan, P. R. Villeneuve, H. A. Haus, J. D. Joannopoulos, Journal of Lightwave Technology **17**(9), 1682 (1999).
[4] P. Achatz, J. A. Garrido, M. Stutzmann, O. A. Williams, D. M. Gruen, A. Kromka, D. Steinmuller, Appl. Phys. Lett. **88**(10), 101908 (2006).
[5] S. Potocky, J. Holovsky, Z. Remes, M. Muller, J. Kocka, A. Kromka, Physica Status Solidi B **251**(12), 2603 (2014).
[6] Y. Chu, N. P. de Leon, B. J. Shields, B. Hausmann, R. Evans, E. Togan, M. D. Lukin, Nano Letters **14**(4), 1982 (2014).
[7] E. Togan, Y. Chu, A. S. Trifonov, L. Jiang, J. Maze, L. Childress, M. D. Lukin, Nature **466**(7307), 730 (2010).
[8] M. Loretz, S. Pezzagna, J. Meijer, C. L. Degen, Applied Physics Letters **104**(3), 033102 (2014).
[9] A. Stacey, D. A. Simpson, T. J. Karle, B. C. Gibson, V. M. Acosta et al., Advanced Materials **24,** 3333 (2012).
[10] A. M. Smith, M. C. Mancini, S. Nie, Nat. Nanotechnol. **4,** 710 (2009).
[11] M. Varga, Z. Remes, O. Babchenko, A. Kromka, Physica Status Solidi B **249**(12), 2635 (2012).
[12] J. Saarilahti, E. Rauhala, Nucl. Instr. Meth. Phys. Res. B **64,** 734 (1992).
[13] M. Mayer, SIMNRA version 6.06, Max-Planck-Institut fur Plasmaphysik, Garching, Germany, 2011. Available at: http://home.rzg.mpg.de/~mam/.
[14] IBANDL, http://www-nds.iaea.org/ibandl/GISA.
[15] R. Ulrich, R. Torge, Appl. Opt. **12**(12), 2901 (1973).
[16] V. Prajzler, M. Varga, P. Nekvindova, Z. Remes, A. Kromka, Optics Express **21**(7), 8417 (2013).
[17] R. Kalish, A. Reznik, S. Prawer, D. Saada, J. Adler, physica status solidi (a) **174**(1), 83 (1999).
[18] O. A. Williams, A. Kriele, J. Hees, M. Wolfer, W. Müller-Sebert, C. E. Nebel, Chemical Physics Letters **495**(1), 84 (2010).
[19] A. C. Ferrari, J. Robertson, Physical Review B **64**(7), 075414 (2001).
[20] P. Galar, B. Dzurnak, M. Varga, M. Marton et al., Opt. Mater. Express **4**(4), 624 (2014).
[21] M. J. Adams, An Introduction to Optical Waveguides, John Wiley & Sons Ltd., 1981.
[22] SRIM, www.srim.org.
[23] P. Djemia, C. Dugautier, T. Chauveau, E. Dogheche, M. I. De Barros, L. Vandenbulcke, Journal of Applied Physics **90**(8), 3771 (2001).
[24] T. Sharda, T. Soga, T. Jimbo, Journal of applied physics **93**(1), 101 (2003).
[25] V. Prajzler, M. Varga, P. Nekvindova, Z. Remes, A. Kromka, Optics express **21**(7), 8417 (2013).
[26] A. Magyar, W. Hu, T. Shanley, et al., Nature Communications **5**, 3523 (2014).
[27] I. Aharonovich, S. Castelletto, D. A Simpson, C. H. Su, A. D. Greentree, S. Prawer, Reports on progress in Physics **74**(7), 07650125 (2011).
[28] I. Aharonovich, E. Neu, Advanced Optical Materials, **2**(10), 911 (2014).

*Corresponding author: pavla.nekvindova@vscht.cz